

ANALYSIS OF TRANSMISSION AND REFLECTION FROM MODIFIED COPLANAR WAVEGUIDE STRUCTURES

Abdelnasser A. Eldek, Atef Z. Elsherbeni, and Charles E. Smith

Department of Electrical Engineering
The University of Mississippi
University, MS 38677

Keywords: Coplanar waveguides, FDTD, Attenuation.

In this paper, several geometries of a class of grounded coplanar waveguide (GCPW) are investigated using the finite difference time domain (FDTD) method, and their losses are computed. A uniform grounded coplanar waveguide (GCPW) structure is used as a reference case for the other non-uniform geometries. First, four geometries are proposed to study the transmission and loss effect of replacing parts of the dielectric substrate with free space. Afterwards, two new geometries are simulated to study the effect of introducing a neck and a gap in the microstrip feeding line, with and without a bridge that connects the two parts of the microstrip feeding line separated with the gap. The effect of adding a PEC cap above the microstrip feeding line, and connecting the two side ground planes, is also studied. The conductor attenuation, the relative power losses, and the feed line impedance are computed and presented.

I. INTRODUCTION

Coplanar waveguide (CPW) structures offer an attractive alternative to conventional microstrip lines in high frequency applications due to many appealing properties. These include low dispersion, high flexibility in the design of characteristic impedance, and ease of connecting shunt lumped elements, or devices without using via holes [1,2]. In addition to these advantages, a GCPW structure provides superior mechanical strength and heat sinking capabilities in comparison with CPWs. Moreover, the conductor backing is particularly useful for multi-layered integrated circuits for beam forming phased array antennas [3], because it provides the required electrical isolation between the different circuit levels.

On the other hand, the presence of conductor backing causes leakage of the power in the transverse direction due to the excitation of parallel plate modes supported by the infinitely extended parallel plates [4]. This type of leakage may produce unwanted crosstalk between neighboring parts of a circuit and unexpected package resonance effects, jeopardizing the use of GCPW as a transmission line [5].

Thus, different structures of GCPW are simulated, using the FDTD numerical method, to study the effect of modifying the basic GCPW configuration on the reflection and transmission properties. A uniform coplanar waveguide structure [6] is used as a reference case for all other non-uniform geometries to produce the incident voltage and current, which are used for calculating the return losses. The preliminary results are verified by a comparison with those presented in [5].

II. PROBLEM FORMULATION

2-1 Basic FDTD Equations

Starting from Maxwell's equations in a 3D domain,

$$\nabla \times \vec{H} = \epsilon \frac{\partial \vec{E}}{\partial t} + \sigma^e \vec{E} + \vec{J} \quad (1)$$

$$\nabla \times \vec{E} = -\mu \frac{\partial \vec{H}}{\partial t} - \sigma^m \vec{H} - \vec{M}, \quad (2)$$

the FDTD technique approximates the derivatives in Maxwell's equations using the second order accurate central difference scheme,

$$\left. \frac{\partial F^n(i, j, k)}{\partial x} \right|_{i\Delta x} = \frac{F^n(i + \frac{1}{2}, j, k) - F^n(i - \frac{1}{2}, j, k)}{\Delta x} \quad (3)$$

$$\left. \frac{\partial F^n(i, j, k)}{\partial t} \right|_{n\Delta t} = \frac{F^{n+1/2}(i, j, k) - F^{n-1/2}(i, j, k)}{\Delta t} \quad (4)$$

Then, Maxwell's equations are transferred into six time updating equations for the electric and magnetic fields, in x , y , and z directions. The general FDTD equations are then given by:

$$\begin{aligned} \vec{E}_u^n(m) = & C_{eue}(m) \vec{E}_u^{n-1}(m) + C_{euh}(m) [\nabla \times \vec{H}]_u^{n-\frac{1}{2}} \\ & - C_{eus}(m) \vec{J}_u^{n-\frac{1}{2}}(m) \end{aligned} \quad (5)$$

$$\begin{aligned} \vec{H}_u^{n+\frac{1}{2}}(m) = & C_{huh}(m) \vec{H}_u^{n-\frac{1}{2}}(m) + C_{hue}(m) [\nabla \times \vec{E}]_u^n \\ & - C_{hus}(m) \vec{M}_u^n(m) \end{aligned} \quad (6)$$

where, u is x , y or z , and (m) is a representation of a cell indices (i, j, k) . All the coefficients, C_{eue} , C_{euh} , C_{eus} , C_{huh} , C_{hue} and C_{hus} , are obtained from [7]. The solution for \vec{E} and \vec{H} is obtained in a gridded computational domain. The computational domain is bounded by an absorbing boundary condition based on the Liao absorbing boundary condition [8].

2-2 Feeding Parameters

The GCPW is fed with a Gaussian pulse waveform $g(t)$. The feeding structure, shown in Fig. 1, offers a uniform distribution of the voltage between the strip and the ground planes. The total voltage between the feed line strip and the ground planes is 1 Volt, and the resistance of the sources between the strip and the ground planes is chosen to be 90Ω for the basic GCPW configuration.

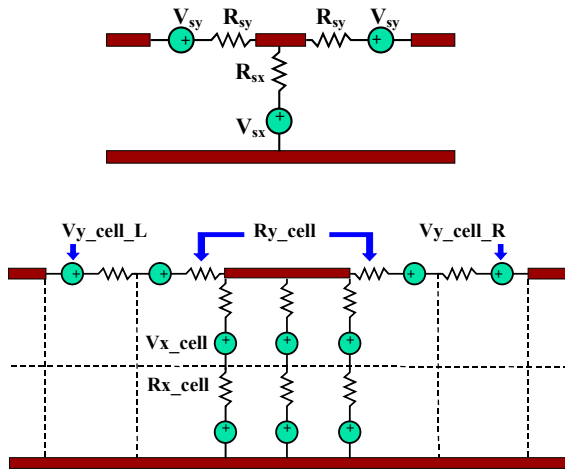


Fig. 1. Mechanism for a GCPW structure.

The parameters of the Gaussian pulse are calculated such that its time domain width is 5% of its maximum value, the turn-on value is e^{-20} of its maximum, while its maximum usable frequency is at 10% of the peak frequency response, and the minimum wavelength corresponding to this frequency contains n_c spatial cells [7], i.e.

$$g(t) = e^{-(t-t_0)^2/\tau^2}, t_0 = 4.5\tau \quad (7)$$

$$f_{\max} = c/n_c \Delta s_{\max} = 1/(2\tau)$$

where Δs_{\max} represents the maximum spatial increment, and n_c is chosen to be 25. The maximum frequency is calculated to be 132 GHz. For this geometry, the feeding point is 5 cells away from the absorbing boundary. The input voltage and current are captured at 10 cells away from the source to avoid any disturbance effects from the source placement in the FDTD grid.

The output voltage and current are captured at 50 cells away from the source and 55 cells away from the absorbing boundary at the end of the GCPW along the z direction, as shown in Fig. 2.

2-3 Parameters of the Structure

The dimensions of the basic structure [5] are illustrated in Fig. 3. In this simulation, 15 cells of free space above the waveguide plane are used. To guarantee stability of the numerical solution, the ratios between dx , dy , and dz must not exceed 1.5, and dt must satisfy the Courant-Friedrichs-Lewy (CFL) condition:

$$\Delta t \leq \frac{1}{c\sqrt{(1/\Delta x)^2 + (1/\Delta y)^2 + (1/\Delta z)^2}} \quad (8)$$

The sampling voltage and current are calculated by integrating the electric and magnetic fields, respectively, with respect to space increment, such that

$$V = -\int \vec{E} \cdot d\vec{l} \approx -\sum E \Delta l \quad \text{and}$$

$$I = \oint \vec{H} \cdot d\vec{l} \approx \sum H \Delta l \quad (9)$$

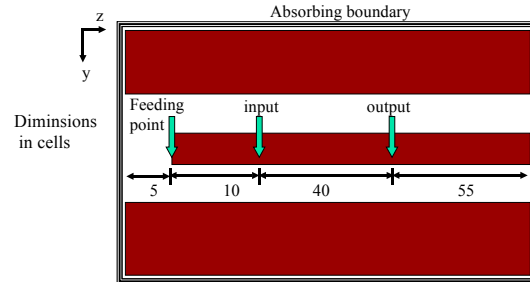


Fig. 2. Feeding and testing points.

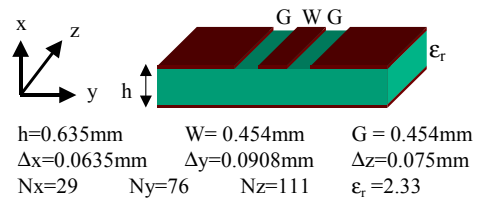


Fig. 3. Basic or reference structure – Case A.

The reflection and transmission, which are represented in terms of the S-parameters S_{11} and S_{21} , respectively, are calculated using the power ratio procedure [7],

$$S_{11} = 10 \log_{10} \left(\left| \frac{V_{refl} I_{refl}^*}{V_{inc} I_{inc}^*} \right| \right) \quad (10)$$

$$S_{21} = 10 \log_{10} \left(\left| \frac{V_{load} I_{load}^*}{V_{inc} I_{inc}^*} \right| \right) \quad (11)$$

where V_{inc} and I_{inc} are voltage and current quantities that are calculated at the input point of the reference case, while V_{refl} and I_{refl} are the differences between the input voltage and current of the current case, and V_{inc} and I_{inc} . The (*) indicates complex conjugate. Finally, the impedance at any point is calculated as

$$Z(f) = V(f)/I(f). \quad (12)$$

2-4 Conductor Loss

The power lost per unit length at high frequencies, due to finite strip conductivity is

$$P_{lc} = \frac{\text{Re}(Z_s)}{2} \int_C |\bar{J}_s|^2 dl, \quad Z_s = (1+j) \sqrt{\frac{\omega\mu}{\sigma}}, \quad (13)$$

where Z_s is the strip surface impedance of the conductor, C is the integration contour that encloses the perimeter of the guide strip, dl is Δy in our case, as shown in Fig. 3, and σ is the conductivity of the conductor, which is assumed to be copper [5.813×10^7 (1/m Ω)]. There are surface currents on both the guide strip and the three ground planes, and the power lost can be computed with the above formula for all conducting surfaces. With a finite conductivity, a surface current density flow on the conducting plane is defined as follows:

$$\bar{J}_s = \hat{n} \times \bar{H}. \quad (14)$$

In our case, $\hat{n} = \pm \hat{x}$, hence,

$$\bar{J}_s = \pm (\hat{z} H_y - \hat{y} H_z), \quad (15)$$

where H_y and H_z are calculated at the z constant planes defined by the output point shown in Fig. 4. In the frequency domain, the integral in equation (13) is approximated as follows:

$$\int_C |J_s(f)|^2 dl \cong \Delta y \sum_m \left[|H_y(m, f)|^2 + |H_z(m, f)|^2 \right] + \Delta y \sum_m \left[|H_{yGround}(m, f)|^2 + |H_{zGround}(m, f)|^2 \right], \quad (16)$$

where H_y and H_z are the magnetic fields at the guide strip and $H_{yGround}$ and $H_{zGround}$ are the magnetic fields at the ground planes. The integer m is the summation index for the magnetic field components associated with the closed contour surrounding the conductors.

2-5 Dielectric Loss

Attenuation in a transmission line or waveguide can be caused by dielectric loss similar to the conductor loss. If α_d is the attenuation constant due to dielectric loss, and α_c is the attenuation constant due to the conductor loss, then the total attenuation constant is $\alpha = \alpha_c + \alpha_d$. The attenuation due to lossy dielectric can be calculated from the absorbed power within the lossy material such as,

$$P_{ld}(f) = \frac{1}{2} \int \sigma |E|^2 dv = \frac{1}{2} \int \left[\sigma_x |E_x|^2 + \sigma_y |E_y|^2 + \sigma_z |E_z|^2 \right] dv, \quad (17)$$

where v denotes the volume containing the lossy material and σ_x , σ_y , and σ_z are the electric conductivities in the x , y , and z directions, respectively.

2-6 Power Losses

In order to study the behavior of the transmission of power, along the strip line, the output power is calculated at several points, Z_{L1} , Z_{L2} , Z_{L3} , Z_{L4} and Z_{L5} , which are shown in Fig.4. The power loss is calculated as a difference between the real part of the input power and that of the output power. The relative power loss is the ratio between the power loss and the real part of input power, which is the same as the transmission loss factor.

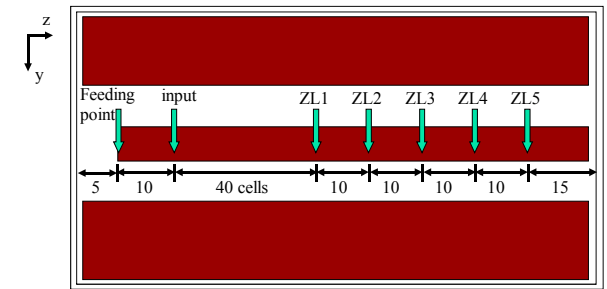


Fig. 4. Points for output power calculations.

The power flow through the cross-section is calculated from the voltage and current at the input point (Fig. 2), such that all resistive losses are disregarded and the disturbances of the source are avoided. The pure input power is then defined as

$$P_{in} = \frac{1}{2} \text{Re} \left[V_{in}(f) I_{in}(f)^* \right]. \quad (18)$$

The attenuation constant due to conductor and dielectric losses can then be computed as [9]:

$$\alpha = \alpha_c + \alpha_d = (P_{lc} + P_{ld})/2P_{in} , \quad (19)$$

and then attenuation per unit length is $-20 \log e^{-\alpha} \text{ dB/m}$.

III. NUMERICAL RESULTS

The geometries used in this paper are shown in Fig. 3 and 5. The transmission coefficient of the reference case A is calculated and compared with the results reported in [5] for verification. A good match is found between the computed and reported results. Afterwards, the other geometries are simulated. The numerical results of the uniform structures, in time domain, show that the voltage and the current attenuate linearly in the direction of z . However, this attenuation decreases with larger free space area in the substrate, as shown in Fig. 6 to 9. The maximum of the input voltage of these structures increases with the increases in the free space area in the substrate, which leads to the increase of input impedance, in general, as shown in Fig. 10(a).

The frequency domain results show that the input and output impedances increase with the introduction of a free space area in the substrate, as shown in Fig 10. The relative power losses increase with frequency, and by increasing the free space areas in the substrate, the relative power losses decrease strongly as shown in Fig. 11(a). The conductor attenuation decreases strongly with free space under the feed line, as shown in Fig. 11(b). The transmission coefficient decreases with frequency, but increases with the increase in the substrate free space area, as shown in Fig. 12(a). Adding a PEC CAP to the reference case also improves transmission, as shown in Fig. 12(b).

Relative to the reference case, the NECK case has almost the same transmission coefficient; however, that of the GAP case behaves like an open circuit at low frequencies and gap coupling improves with increasing frequency, as shown in Fig. 12(c). As expected, the NECK case has smaller reflection than the GAP case, specially at lower frequencies as shown in Fig. 12(d). When adding a bridge, both transmission and reflection coefficients improve, as shown in Fig. 12(e) and (f) for frequencies up to 80 GHz for this GCPW parameter.

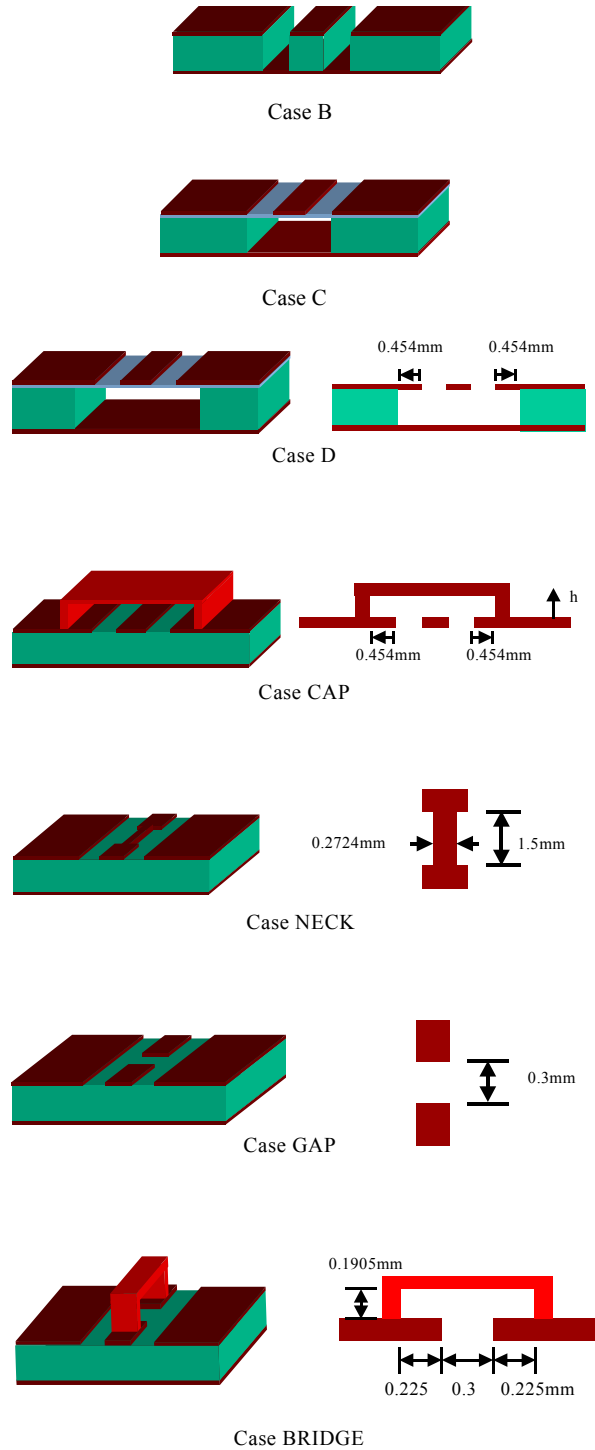


Fig. 5. GCPW configurations.

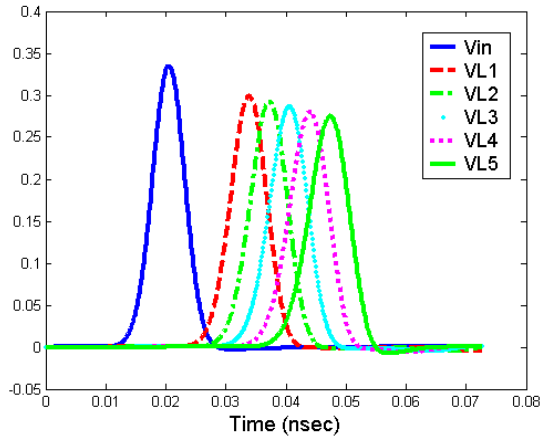


Fig. 6. Input and output voltage for case A.

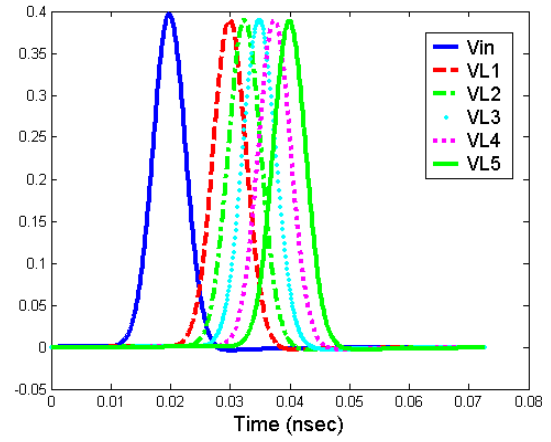


Fig. 9. Input and output voltage for case D.

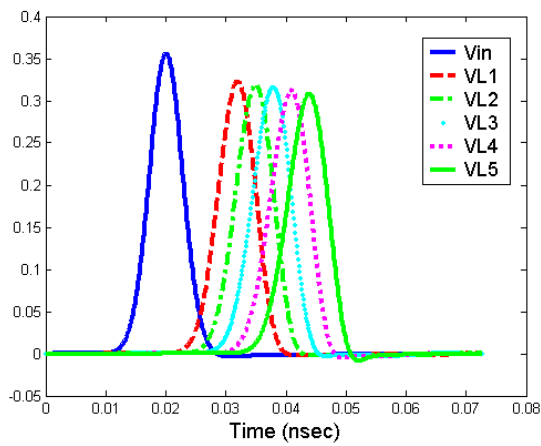


Fig. 7. Input and output voltage for case B.

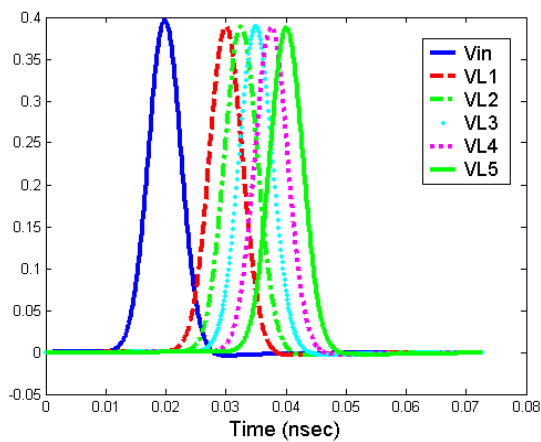


Fig. 8. Input and output voltage for case C.

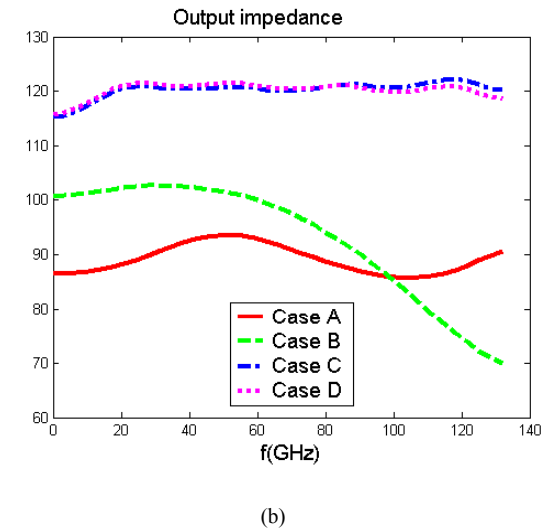
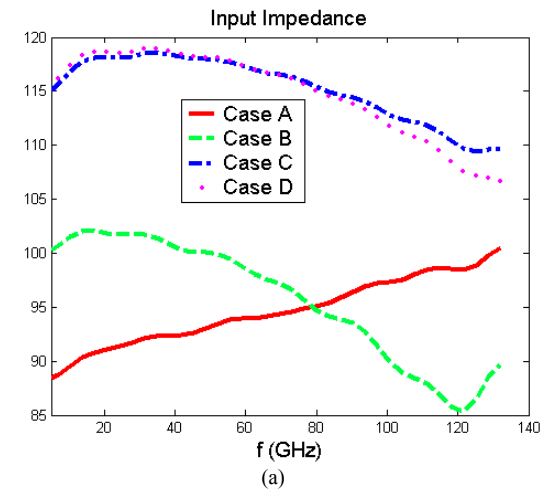
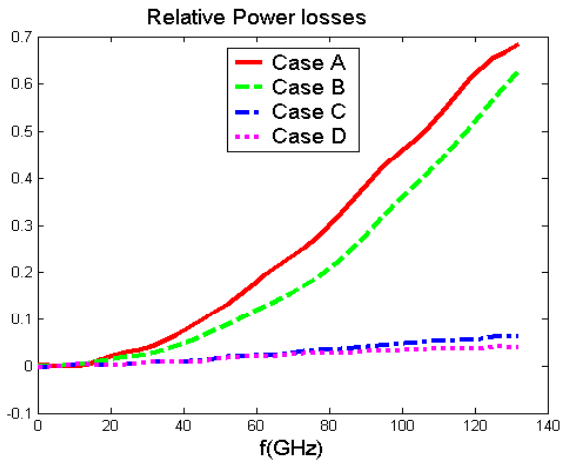
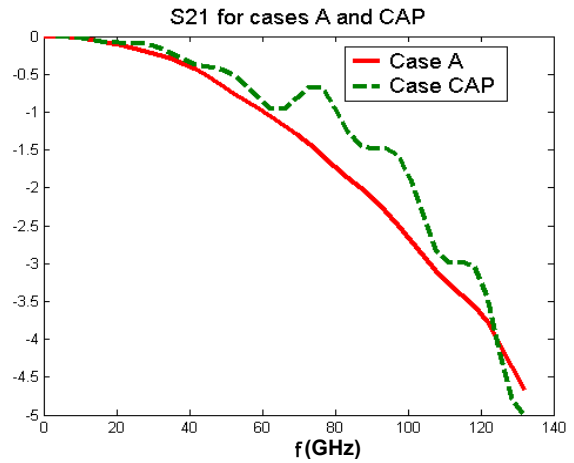


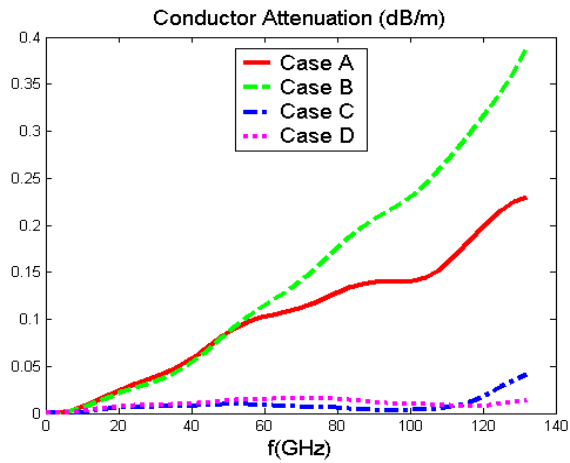
Fig. 10. (a) Input impedance. (b) Output impedance.



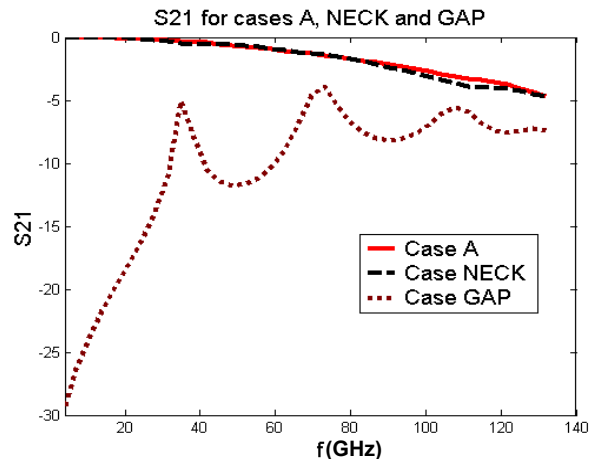
(a)



(b)

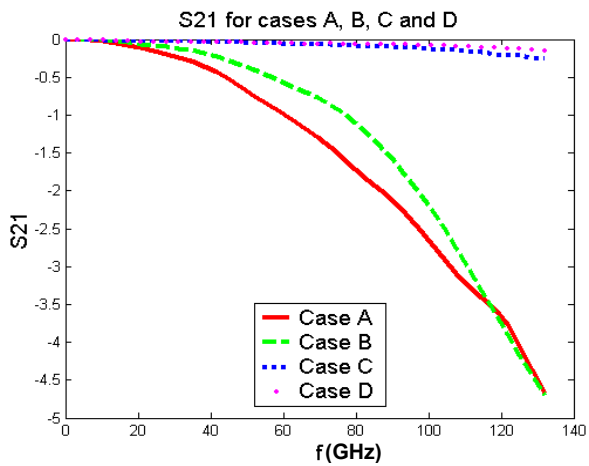


(b)

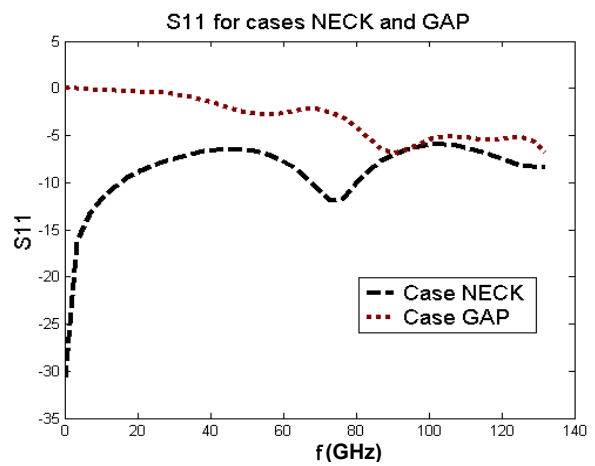


(c)

Fig. 11. (a) Relative power losses (b) Conductor attenuation.



(a)



(d)

Fig. 12. S11 and S21 comparisons.
 (a) S21 for cases A to D (b) S21 for cases A and CAP
 (c) S21 for cases A, NECK and GAP (d) S11 for cases NECK and GAP

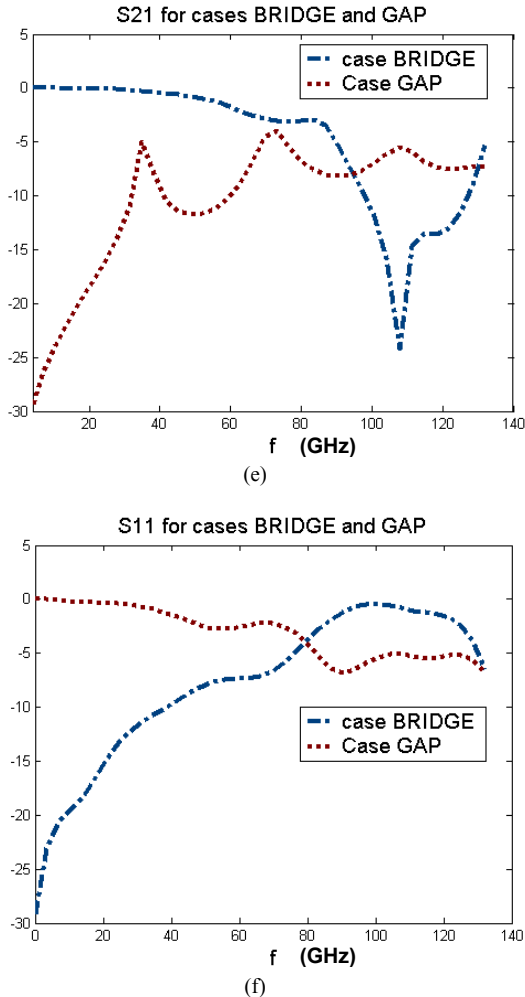


Fig. 12. S11 and S21 comparisons.

(e) S21 for cases BRIDGE and GAP (f) S11 for cases BRIDGE and GAP

IV. CONCLUSION

Different configurations of GCPW are proposed and simulated to study the effect of changing the geometrical parameters on the device losses and input impedance. Four geometries are used to study the effect of replacing parts of the dielectric substrate with free space. It is seen that the transmission coefficient and power losses improve, and both input and output impedances increase when increasing the free space area. The conductor attenuation decreases with free space under the feed line. Adding a PEC cap over the feed line improves the transmission. In the gapped feed line, adding a bridge improves both transmission and reflection. These GCPW configurations have been investigated primarily for use in low-loss power combiners and dividers for use in phased array antenna applications. Other related applications include the

design of hybrid RFIC and MMIC systems on semiconductor chips.

V. REFERENCES

- [1] C. P. Wen, "Coplanar waveguide: a surface strip transmission line suitable for nonreciprocal gyromagnetic device applications," *IEEE Trans. Microwave Theory Tech.*, vol. MTT-17, pp. 1087-1090, Dec. 1969.
- [2] N. I. Dib, W. P. Harokopus Jr., G. E. Ponchak, and L. P. B. Katheti, "A comparative study between shielded and open coplanar waveguide discontinuities," *International Journal of Microwave and Millimeter-Wave Computer-Aided Engineering*, vol. 2, no. 4, pp. 331-341, 1992.
- [3] N. K. Das and D. M. Pozar, "Multipoint scattering analysis of multilayered printed antennas fed by multiple feed ports, part I: theory; part II: applications," *IEEE Trans. Antennas Propagat.* vol-AP 40, pp. 469-491, May 1992.
- [4] H. Shigeswa, M. Tsuji and A. A. Oliner, "Dominant mode power leakage from printed-circuit waveguide," *Radio Sci.*, vol. 26, pp. 559-564, Mar./Apr. 1991.
- [5] Z. Ma and E. Yamashita, "Comparative studies of discontinuities in single and double layered conductor-backed coplanar waveguides," *IEEE MTT-S Int. Microwave Symp. Dig.*, vol. 3 pp. 1803-1806, 1996.
- [6] Y. Liu and T. Itoh, "Control of leakage in multilayered conductor-backed coplanar structures," *IEEE MTT-S Int. Microwave Symp. Dig.*, pp. 141-144, 1994.
- [7] A. Z. Elsherbeni, "The finite difference time domain for electromagnetic applications," class notes, Electrical Engineering Department, The University of Mississippi, Jan. 2002.
- [8] Z. P. Liao, H. L. Wong, B. -P. Yang, and Y. -F. Yuan, "A transmitting boundary for transient wave analysis," *Scientia Sinica, Series A*, vol. 27, pp. 1063-1076, 1984.
- [9] D. M. Pozar, *Microwave Engineering*. New York, NY: John Wiley, 1998.



Abdelnasser Eldek received an honor B.Sc. degree in Electronics and Communications Engineering from Zagazig University, Zagazig, Egypt, in 1993 and an M.S. degree in Electrical Engineering from Eindhoven University of Technology, Eindhoven, The Netherlands, in 1999.

He was a research assistant with the Electronic Research Institute, in Cairo, Egypt, from 1995 to 1997, and from 1997 to 1999 he was a Master student at Eindhoven University of Technology with the cooperation of

Philips Center For Technology and Fontys University for professional education, Eindhoven. From 1999 to 2000 he was assistant teacher in the Industrial Education College, Beni Suif, Egypt. He is currently working towards his Ph.D. degree and is a research assistant at the Department of Electrical Engineering, the University of Mississippi.



Atef Z. Elsherbeni received an honor B.Sc. degree in Electronics and Communications, an honor B.Sc. degree in Applied Physics, and a M.Eng. degree in Electrical Engineering, all from Cairo University, Cairo, Egypt, in 1976, 1979, and 1982, respectively, and a Ph.D. degree in Electrical Engineering from Manitoba University, Winnipeg, Manitoba, Canada, in 1987. He was a Research Assistant with the Faculty of Engineering at Cairo University from 1976 to 1982, and from 1983 to 1986 at the Electrical Engineering Department, Manitoba University. He was a part time Software and System Design Engineer from March 1980 to December 1982 at the Automated Data System Center, Cairo, Egypt. From January to August 1987, he was a Post-Doctoral Fellow at Manitoba University. Dr. Elsherbeni joined the faculty at the University of Mississippi in August 1987 as an Assistant Professor of Electrical Engineering. He advanced to the rank of Associate Professor on July 1991, and to the rank of Professor on July 1997. He spent his first sabbatical term in 1996 at the Electrical Engineering Department, University of California at Los Angeles (UCLA).

Dr. Elsherbeni received the 2002 IEEE Region 3 Outstanding Engineering Educator Award, The 2002 School of Engineering Outstanding Engineering Faculty Member of the Year Award, the 2001 Applied Computational Electromagnetic Society (ACES) Exemplary Service Award for leadership and contributions as Electronic Publishing managing Editor 1999-2001, the 2001 Researcher/Scholar of the year award in the Department of Electrical Engineering, The University of Mississippi, and the 1996 Outstanding Engineering Educator of the IEEE Memphis Section. His professional interests include scattering and diffraction of electromagnetic waves, numerical techniques, antennas, remote sensing, and computer applications for electromagnetic education. He has published 57 technical journal articles and 12 book chapters on applied electromagnetics, antenna design, and microwave subjects, and presented over 170 papers at professional conferences. Dr. Elsherbeni is a senior member of the Institute of Electrical and Electronics Engineers (IEEE). He is the Editor in-Chief for the Applied Computational Electromagnetic Society (ACES) Journal and the electronic publishing managing editor of ACES. His honorary memberships include the Electromagnetics Academy and the Scientific Sigma Xi Society. He serves on the editorial board of the Book Series on Progress in Electromagnetic Research, the Electromagnetic Waves and Applications Journal, and the Computer Applications in Engineering Education Journal. He was the Chairman of the Educational Activity Committee for the IEEE Region 3 Section from 2000 to 2001. Dr. Elsherbeni's home page can be found at

<http://www.ee.olemiss.edu/~atef> and his email address is Elsherbeni@ieee.org.



Charles E. Smith was born in Clayton, AL, on June 8, 1934. He received the B.E.E., M.S., and Ph.D. degrees from Auburn University, Auburn, AL, in 1959, 1963, and 1968, respectively. While pursuing his advanced degrees from 1959 to 1968, he was employed as a Research Assistant with Auburn University Research Foundation.

In late 1968, he accepted the position of Assistant Professor of Electrical Engineering with The University of Mississippi, University, MS, and he advanced to the rank of Associate Professor in 1969. He was appointed Chairman of the Department of Electrical Engineering in 1975, and he is currently Professor and Chair of this department. He has directed and is heavily involved in the development of The University's current circuits, electronics, HF and microwave, computer-aided-design, and digital systems courses and laboratories. His main areas of interest are related to the application of electromagnetic theory to microwave circuits, antennas, measurements, RF and wireless systems, radar, digital and analog electronics, and computer-aided design. His recent research has been on the application of numerical techniques to microstrip transmission lines, antenna measurements in lossy media, measurement of electrical properties of materials, CAD in microwave circuits, radar designing, and data acquisition using network analyzers. Dr. Smith has published widely in these areas and has over 200 total publications including journal papers, technical reports, book chapters, and paper presentations. He has advised, or co-advised, 46 M.S. thesis and PH.D dissertations, and has received 6 awards for outstanding teaching and scholarship at The University of Mississippi.

He is a Life Senior Member of the IEEE and is a member of the IEEE Antennas and Propagation Society, IEEE Microwave Theory and Techniques Society, IEEE Education Society, American Society of Engineering Education, Phi Kappa Phi, Eta Kappa Nu, Tau Beta Pi, and Sigma Xi.